# CONFINED BOILING OF n-PENTANE IN A HORIZONTAL SPACE

E. M. CARDOSO*, J. C. PASSOS*, B. STUTZ**, M. LALLEMAND**

* Departamento de Engenharia Mecânica, LEPTEN/Boiling, Universidade Federal de Santa Catarina, Cx. P. 476, 88010-900 Florianópolis, SC, Brazil.
** Centre Thermique de Lyon, Institut National des Sciences Appliquées de Lyon – UMR – CNRS, 5008 20, Av. Albert Einstein, 69621 Villeurbanne cedex, France

**ABSTRACT**

This paper presents new experimental results for saturated nucleated boiling of n-Pentane on a heated surface facing upward, at atmospheric pressure, for different degrees of confinement, $s$ = 0.2 and s = 13mm. Comparisons with results from the literature, together with visualizations of the tests and analysis of the experimental data, allowed the improvement of the experimental apparatus. The results show the enhancement of boiling heat transfer for $s$ = 0.2mm and a heat flux below 140kW/m$^2$ and a decrease in $h$ only above a heat flux of 140kW/m$^2$, leading to an increase in the dry area on the heated surface.

**Keywords:** Nucleate boiling, confined boiling, dryout heat flux.

## INTRODUCTION

The development of new cooling technologies associated with a reduction in manufacturing and installation costs requires the dissipation of increasing heat flux. The heat transfer associated with the phase change continues to be studied with the aim of achieving high heat transfer coefficients, for applications such as the cooling of electronic components or as a basis for diverse energy conversion systems that rely on the efficiency of the evaporator.

An in-depth analysis is required in the case of confined nucleate boiling in order to perfect its use as an intensification technique and also to minimize the risks associated with confinement when it is imposed on a design, because it can cause problems linked to the premature occurrence of critical heat flux, which represents the limit of operation of the system in the nucleate boiling regime.

The effect of the confinement on the bubbles can be characterized by a dimensionless parameter known as the Bond number, *Bo*, defined as the ratio of the characteristic length to the confined space, $s$, and the capillary length, $L$. The latter is proportional to the detachment diameter of the vapor bubble in a pool and defined as [1]:

$$L = \sqrt{\frac{\sigma}{g(\rho_l - \rho_v)}} \tag{1}$$

where $\sigma$, $g$, $\rho_l$ and $\rho_v$ represent the surface tension, the acceleration due to gravity, the liquid density and the vapor density, respectively.

According to Eq. (2), a decrease in the superheating $\Delta T_{sat} = (T_w - T_{sat})$ for the same heat flux, $q$, causes an increase in the heat transfer coefficient, $h$.

$$h = \frac{q}{\Delta T_{sat}} \tag{2}$$

Several studies have focused on the effects of contact angle, thermophysical properties, dimension, shape, thickness, orientation in space, roughness and the microstructure of the boiling surfaces.

The objective of this study is the experimental investigation of n-Pentane in confined and unconfined spaces, with pool boiling heat transfer on an upward facing surface and under saturated conditions. The motivation of this study is the understanding of the mechanisms and effects under the nucleate boiling regime.

## LITERATURE REVIEW

The increase in the heat transfer coefficient when *Bo*<1 is explained by the evaporation of a thin liquid film, which is present between the heated surface and the base of the deformed bubble [2]. For a low Bond number, as a consequence of the coalescence phenomenon, the bubble becomes large and deformed allowing an increase in the bubble area pressed against the heated wall. According to Straub [3], at the base of the bubble a thin liquid film called the microlayer is attached to the surface by intermolecular attractive forces between the liquid and the surface and because of these, the film does not evaporate completely. Only a high superheating will evaporate the microlayer, with a dry area then forming and the heat transfer coefficient slowly decreasing.

When *Bo*>1, the bubbles are isolated and the boiling mechanism tends to be similar to that on an upward facing heated surface in a liquid pool. However, for a downward facing heated surface there is an increase in the heat transfer coefficient because of the thicker thermal layer that increases the nucleation site density [4, 5].

The boiling crisis, when the imposed heat flux attains the maximum value for the nucleate boiling regime, before the decrease in the heat transfer coefficient, for an infinite upward facing heated surface cooled by a liquid pool, is calculated by the Zuber's equation, [1]:

$$q_{máx,Z} = 0{,}131\rho_v^{0,5} h_{lv}\left[\sigma g(\rho_l - \rho_v)\right]^{\frac{1}{4}} \quad (3)$$

The literature contains a number of publications that report studies on the factors that affect pool boiling heat transfer. These include the effects of surface characteristics such as thermophysical properties, dimensions, etc., and also the thermophysical properties of the working fluid.

The effects of cavity size, shape, and density of nucleation have been those most widely investigated [6]. Cavity radius and depth, contact angle of the fluid, and initial fluid penetration velocity are important parameters determining the stability of a cavity during boiling.

Some experiments have shown that, with increasing surface roughness, starting from a smooth polished surface, $h$ increases and reaches a maximum value; after this point, a further increase in surface roughness has no effect on the boiling heat transfer [7].

In the case of a rough surface that has quite a large number of potential vapor generating centers, the wall thermal conductivity does not significantly affect the boiling heat transfer.

Wang and Dhir [8] conducted experiments with water boiling at atmospheric pressure on vertical copper surfaces with different wetabilities (contact angles of 90°, 35° and 18°). They concluded that the number of active vapor generating centers decreased as the wettability of the boiling surface increased, or as the values of the contact angle decreased.

The effect of boiling surface orientation on $h$ is noticeable. Kang [9] conducted experiments with pool boiling on horizontal, inclined, and vertical tubes and found that the orientation effect on the heat transfer could be significant. According to his findings, the $h$ value is higher for an inclined tube (about 45° from the horizontal plane) compared to horizontal and vertical orientations. This effect seems to be due to decreased bubble slug formation on the boiling surface and improved liquid access to the surface.

This trend was also observed by Nishikawa *et al*. [10], who studied the influence of the orientation of the heated surface, from 0° (horizontal upward facing heated plate) to close to 180° (downward facing heated plate) and the heat flux on water nucleate boiling, at atmospheric pressure. Their results indicated that for low heat flux values and $\theta < 120°$, the heat transfer is controlled by the agitation of isolated vapor bubbles. However, for $\theta > 150°$, the heat transfer is controlled by the removal of the superheated thermal layer when the vapor bubble slides over the surface and by the heat of vaporization due to the liquid film vaporization under the vapor bubble when it covers the surface. For high heat fluxes, the mechanisms associated with the movement of the vapor bubble are not influenced by orientation of the surface.

You *et al.* [11] conducted FC-72 and R-113 saturated pool boiling experiments at atmospheric pressure, using a 0.13 mm diameter chromel wire and 0.51 mm diameter platinum cylinder. The properties of the liquid affect the wall superheating values but the material effect was less significant than the surface microgeometry for highly wetting dielectric fluids. The capacity of such fluids to flood microcavities induces large superheats at incipience.

Liang and Yang [12] illustrated the fundamental importance of the contact angle comparing boiling incipience of n-Pentane on a flat copper surface and on a porous graphite/copper surface. The use of graphite/copper reduced considerably the hysteresis at boiling incipience, by increasing the number and the size of the nucleation sites and their capacity to preserve the vapor nucleus. The authors explained these results through the contact angle, 2° for the n-pentane on copper versus 35° for the n-pentane on graphite.

## EXPERIMENT

Figure 1 shows the experimental set up, consisting of a boiling chamber (8) installed in the center of an external chamber (9), both assembled between two horizontal stainless steel plates of 200 x 200 x 10 mm (12 and 13). The boiling chamber is a vertical glass tube with a 90 mm inner diameter and 175 mm height, the test section and the working fluid being inside. The external chamber has a square cross section of 170x170 mm and transparent lateral walls of plexy-glass (9). The test condition temperature of the working fluid is imposed by a forced flow of water in the space created between the glass tube of the boiling chamber and the plexy-glass wall of the external chamber. The water temperature is controlled by a cryostat. Inside the boiling chamber, in the upper part, there is a serpentine condenser (7) cooled by water whose temperature is controlled by a second cryostat. The boiling chamber is equipped with a pressure transducer (3) and valves (2 and 6). Two type-K thermocouples (4) in the liquid and one in the vapor, allow the monitoring of the test condition temperatures, which are controlled by cold water flowing inside the serpentine (7).

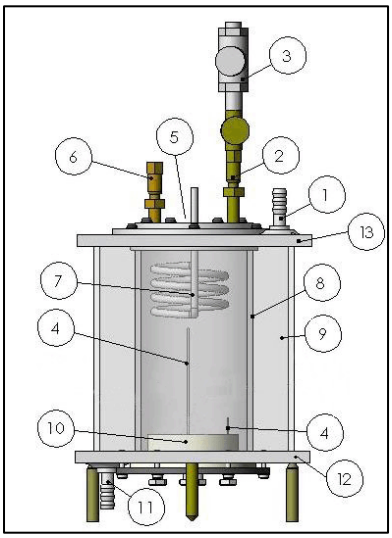


Figure 1. Scheme of the experimental apparatus:
1) Bath water inlet; 2) Valve; 3) Pressure transducer; 4) Thermocouples; 5) Plexy-glass window; 6) Valve; 7) Condenser; 8) Boiling chamber; 9) Plexy-glass chamber; 10) Test section; 11) Bath water outlet; 12) and 13) Stainless steel plates.

The test section, Fig. 2, consists of a copper block of 12 mm diameter and 60 mm height cylinder, isolated on its perimeter with Teflon®. The experiments are performed using n-Pentane as the working fluid under saturated conditions at $p$ = 1bar ($T_{sat}$ = 35.8°C). The capillary length is close to $L$ = 1.6mm. The section test is heated by a cartridge heater of 177Ω, Fig. 2, imbedded in the sample. This resistance must be sufficient to reach the critical heat flux which, according to Eq. (3), is 243kW/m$^2$ for n-Pentane.

Four type-K thermocouples, fixed in the cylindrical part of the copper block, are used to determine the wall temperatures and the heat flux.

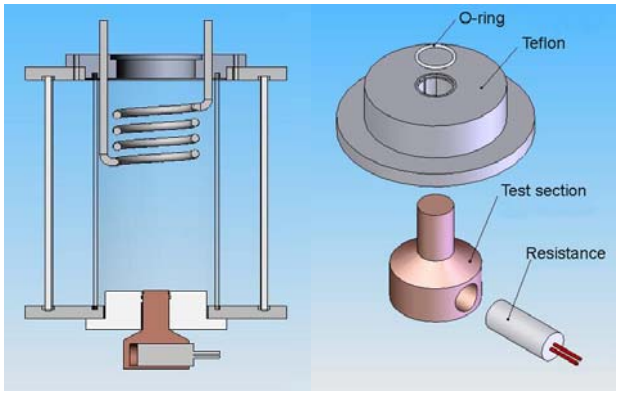


Figure 2. View of test section assembly.

The confined element, Fig. 3, consists of a transparent acrylic piece fixed to an aluminum support, and this in turn is fitted to the test section. This conical unheated plate is placed parallel to the heated surface (45° cone angle and 12mm diameter at the bottom). Inside the upper part of the boiling chamber there is a transparent plexy-glass window, allowing the visualization of the boiling phenomenon on the heated surface.

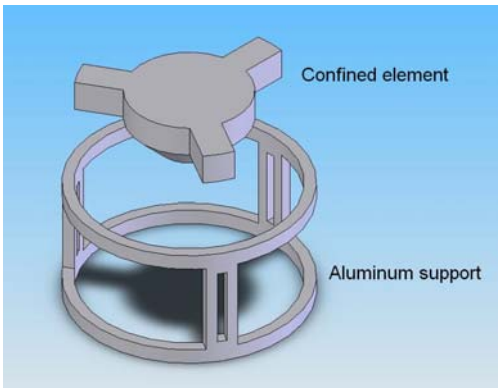


Figure 3. View of confined element.

Figure 4 shows a schematic drawing showing the cryostat, power source, data aquisition system and the computer.

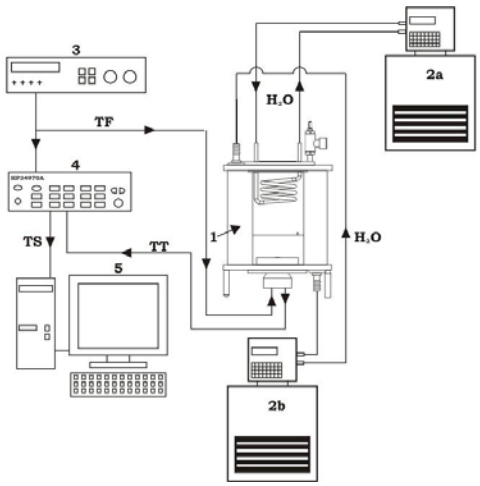


Figure 4. Schematic drawing of the apparatus.

1) Boiling Chamber; 2a) Serpentine Cryostat; 2b) Liquid Circulation Cryostat; 3) Power Source; 4) Data Aquisition System; 5) Computer; TS) All Signals; TT) Thermocouples and pressure transducer signals; TF) Power source signal.

**Experimental Procedure**

Before each test run the working fluids were heated to very close to the saturation temperature in order to degas them. No evidence of significant amounts of gas dissolved in the working liquids was detected in the boiling curves.

A vacuum was created in the boiling chamber, before each series of measurements, which was then fed with the working fluid. By setting the temperature of the water bath, the test conditions represented atmospheric pressure and the saturation temperature. These conditions were regulated by monitoring the pressure and the temperature inside the boiling chamber. Once the test conditions had stabilized, the heat flux was imposed in the range of 15 to 190 kW/m².

The experimental procedure was programmed in LABVIEW and each test had a 180s duration for each imposed heat flux followed by an interval of 300s with the power supply turned-off. Only the temperature data for the last 90s of the test interval were acquired, at a rate of 3 points/s.

The test section was polished using #600 emery paper and the surface was then cleaned using acetone and dried with an air jet. This procedure was repeated before each series of measurements.

The uncertainties of temperature and heat flux were ± 0.2°C and 2.2%, respectively. The experimental uncertainty for the heat transfer coefficient, in nucleate boiling, was 2.4% for heat fluxes near 180kW/m$^2$, and 2.9% for a heat flux of 15kW/m$^2$.

**RESULTS**

**Partial Boiling Curves**

Figure 5 shows the effect of the confinement on the partial boiling curve, at saturation temperature, for n-pentane, for $s$ = 0.2 and 13 mm. The capillary length, Eq. (1), is approximately 1.6mm. For these values of $s$, the Bond number is equal to 0.13 and 8.35, respectively. We can observe for $s$ = 0.2 mm, a particular dependence on the heat transfer coefficient (or $\Delta T$) of $s$ and $q$.

For $s$ = 0.2mm and heat fluxes lower than 140kW/m$^2$, the experimental points are shifted to the left compared with the case of $s$ = 13mm, characterizing an enhancement in the heat transfer for the confined case. However, for a heat flux higher than 140kW/m$^2$ the wall temperature increases, which led us to consider the possibility of starting the dryout heat flux earlier than in the case with $s$ = 13mm. Due to this very thin gap, corresponding to a Bond number of 0.13, the bubbles are deformed and the frequency of bubble detachment is not sufficient to cool the heated surface.

For the cases with a very high level of confinement, $s \leq$ 0.5mm, the enhanced boiling is a consequence of the deformed bubbles which increase the area of the liquid film between the vapor bubble and the wall, allowing an efficient heat transfer, as explained by Katto [13] and Ishibashi and Nishikawa [2].

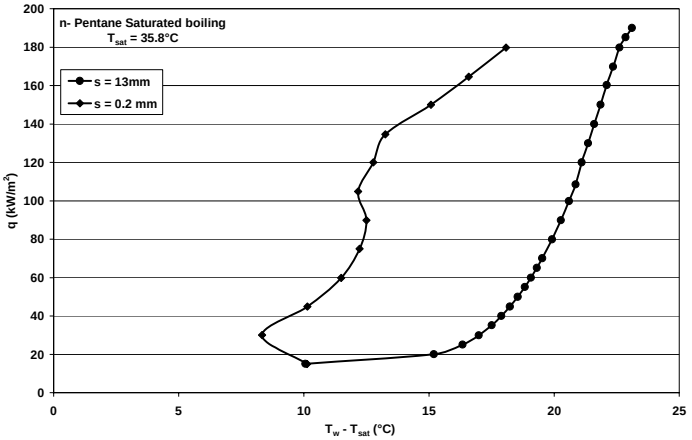


Figure 5. Partial boiling curves for n-Pentane.

Figure 6 shows the heat transfer coefficient, $h = q/(T_w - T_{sat})$, against the heat flux for saturated n-pentane. For the case with confinement we can observe a decrease in $h$ when $q$ is higher than 140kW/m$^2$.

The high values for heat flux can be explained by thermophysical properties of n-Pentane, as mentioned in Peng *et al*. [14]. These authors found that liquids with greater liquid/vapor density differences, higher latent heats and larger thermal diffusion coefficients need higher heat fluxes to initiate nucleation.

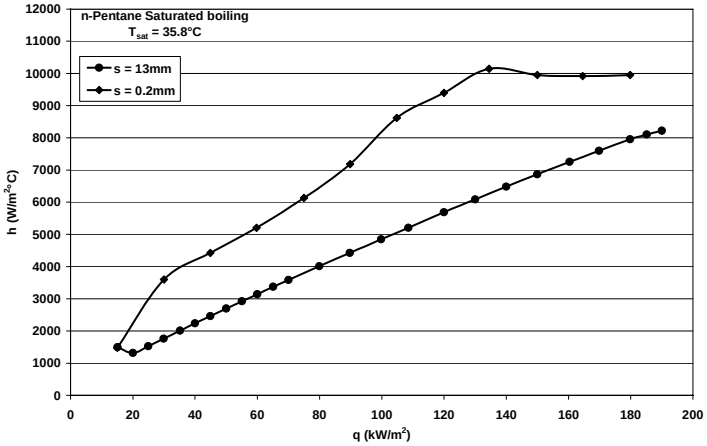


Figure 6. Confinement effect on the heat transfer coefficient against the heat flux, for $s$ = 0.2 and 13mm.

## Dryout Heat Flux

Figures 7 and 8 show the diagrams representing the method used to determine the experimental dryout heat flux, DHF, and the wall superheating at the beginning of the wall dryout, $\Delta T_{DHF}$, for $s$ = 0.2mm. In Fig. 7, the horizontal line slope on the maximum point of the curve of $h$ versus $q$, obtained by fitting the experimental points, allows the determination of $h_{DHF}$, and the corresponding heat flux, $q_{DHF}$. Taking a horizontal line from $q_{DHF}$ and crossing the experimental partial boiling curve $q$ x $\Delta T_{sat}$, Fig. 8, the corresponding experimental wall superheating $\Delta T_{DHF}$, can be obtained at the point at which the abscissa is intercepted by the vertical line.

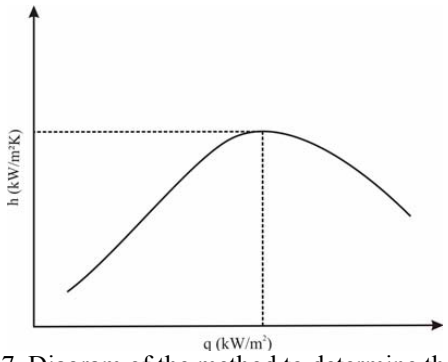


Figure 7. Diagram of the method to determine the $q_{DHF}$.

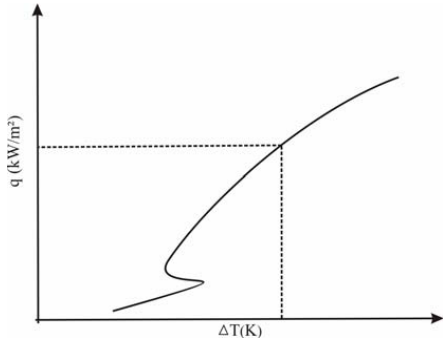


Figure 8. Diagram of the method to determine the $\Delta T_{DHF}$.

Table 1 gives the experimental values of $q_{DHF}$, $h_{DHF}$, $\Delta T_{DHF}$ (determined from Figs. 5 and 6) and the ratio between $q_{DHF}$ and the theoretical value of $q_{max,Z}$, calculated by Eq. (3).

Table 1. Experimental values for n-Pentane.

| $s$ (mm) | $q_{DHF}$ (kW/m$^2$) | $h_{DHF}$ (W/m$^2$°C) | $\Delta T_{DHF}$ (°C) | $q_{DHF}/q_{máx,Z}$ (%) |
|---|---|---|---|---|
| 0.2 | 134.5 | 10147 | 13.3 | 55.8 |

The theoretical value of $q_{máx,Z}$ for n-Pentane is 241.24kW/m$^2$ and the value of $q_{DHF}/q_{máx,Z}$ is 55.8%.

For $s$ = 13.0mm, the graphs indicate unconfined boiling, where the heat transfer coefficient increases as the heat flux increases. In this study, due to the technical limitations of the heating system, only the dryout heat flux for the confined case was obtained.

## Visualization

A visualization study of the n-pentane nucleate boiling regime was carried out, at atmospheric pressure and saturation temperature, for the configuration of an upward facing heated surface, with the higher degree of confinement, $s$ = 0.2mm, and without confinement, $s$ = 13mm.

Figures 9 and 10 show the photographs of boiling for $s$ = 0.2 and 13mm, for two heat fluxes, 45 and 180kW/m$^2$. For $s$ = 13mm there is no effect of confinement and for low heat flux there are few active nucleation sites. The majority of bubbles on the heated surface are isolated.

For $s$ = 0.2mm we can observe that a big bubble is formed by coalescence of small bubbles that apparently escape the confined channel sliding of the small bubbles.

As interpreted by Passos *et al*. [15], after departure of this big bubble a front of cold liquid enters the channel and cools the surface. This mechanism is dependent on the conditions imposed by the geometric characteristics of the heated surface and its support. Thus, the ratio between the diameters of the support and the test section can influence the residence time of the bubble in the channel.

(a) $T_w = 10.1°C$ (b) $T_w = 18.2°C$

Figure 9. Effect of the confinement for $q = 45kW/m^2$: (a) $s = 0.2mm$ and (b) $s = 13mm$.

These images allow us to compare the differences in the configurations of the liquid-vapor interface. For $q = 45kW/m^2$, the temperature of the surface for $s = 0.2mm$ is lower than for $s = 13mm$, indicating an enhancement of the boiling when $Bo < 1$.

(a) $T_w = 18.0°C$ (b) $T_w = 22.6°C$

Figure 10. Effect of confinement for $q = 180kW/m^2$: (a) $s = 0.2mm$ and (b) $s = 13mm$.

In Fig. 10, on increasing the heat flux to $180kW/m^2$ the difference between the surface temperatures for $s = 0.2$ and 13mm decreased, indicating a process of dryout in the confined case. Also, we can observe an increase in the number of bubbles for $s = 13mm$, indicating the efficiency of the boiling process.

## CONCLUSIONS

An experimental analysis was presented on the effect of confinement on the partial n-pentane saturated boiling curves for a copper block of diameter 12mm and an upward facing heated surface. The main results are the following:

(i) As a general trend the heat transfer coefficient increases when the confinement increases, corresponding to a decrease in the distance between the heated surface and an unheated horizontal surface.

(ii) The value of $q_{DHF}/q_{máx,Z}$ was 55.8% and the trend of a decrease in the dryout heat flux in the confined case was only partially found in this study. This uncertainty in the tendency of DHF is attributed to the chaotic phenomenon of coalesced bubble retention in a confined space.

(iii) The visualization for n-pentane shows, for $s = 13mm$, no effect of confinement and for low heat flux most of the vapor bubbles appear at the copper/Teflon interface. For $s = 0.2mm$, a big bubble was formed by coalescence of small bubbles that escaped the confined channel sliding. Increasing the heat flux to $180kW/m^2$, the difference between the surface temperatures for $s = 0.2$ and 13mm decreased, indicating a process of dryout in the confined case.


## ACKNOWLEDGEMENTS

The authors are grateful for the support of the Brazilian Space Agency (AEB), CAPES and the Research Council of Brazil (CNPq) in performing this study. The authors extend their thanks to Mr. D. R. Souza and Mr. A. Dalmaz for an important contribution to the laboratory work.


## NOMENCLATURE

| Symbol | Quantity | SI |
|---|---|---|
| g | acceleration due to gravity | $m/s^2$ |
| h | heat transfer coefficient | $kW/m^2°C$ |
| $h_{lv}$ | latent heat of vaporization | kJ/kg |
| L | capillary length | mm |
| q | heat flux | $kW/m^2$ |
| s | gap of confinement | mm |
| T | temperature | °C |

***Greek symbols***

| | | |
|---|---|---|
| ΔT | wall superheating | K, °C |
| θ | slope angle | ° |
| ρ | density | $kg/m^3$] |
| σ | surface tension | N/m |

***Subscripts***

| | |
|---|---|
| CHF | critical heat flux |
| DHF | dryout heat flux |
| l | liquid |
| lv | liquid-vapor |
| sat | saturation |
| v | vapor |
| w | wall |

## REFERÊNCIAS


[1] V.P. Carey, Liquid-Vapor Phase-Change Phenomena, *Taylor & Francis*, USA, 1992.

[2] E. Ishibashi and K. Nishikawa, Saturated Boiling Heat Transfer in Narrow Spaces, *Int. J. Heat Mass Transfer,* vol. 12, pp. 863-894, 1969.

[3] J. Straub, The role of surface tension for two-phase heat and mass transfer in the absence of gravity, *Experimental Thermal Fluid Science*, vol.9, pp.253-273, 1994.

[4] J.C. Passos, F.R. Hirata, L.F.B. Possamai, M. Balsamo and M. Misale, Confined Boiling of FC-72 and FC-87 on a Downward Facing Heating Copper Disk, *Int. J. Heat and Fluid Flow*, vol. 25 (2), pp. 313-319, 2004.

[5] E.M. Cardoso, Experimental Study of Confined Nucleate Boiling, Master Science Dissertation, Graduate Program on Mechanical Engineering, in Portuguese, Federal University of Santa Catarina, Brazil, pp. 1-96, 2005.

[6] R. J., Benjamin and A. R., Balakrishnan, Nucleation Site Density in Pool Boiling of Saturated Pure Liquids: effect of surface microroughness and surface and liquid physical properties, *Experimental Thermal and Fluid Science*, vol.15, pp. 32-42, 1997.

[7] A., Luke, Thermo and Fluid Dynamics in Boiling, connection between surface roughness, bubble

formation and heat transfer, *5th International Boiling Heat Transfer Conference*, Montego Bay, Jamaica , 4-8 May, 2003.

[8] C.H., Wang and V.K., Dhir, Effect of surface wettability on active nucleation site density during pool boiling of water on a vertical surface, *Transactions of ASME – Journal of Heat Transfer*, vol.115, pp. 659-669, 1993.

[9] M.G. Kang, Effect of tube inclination on pool boiling heat transfer, *Transactions of ASME – Journal of Heat Transfer*, vol. 122, pp. 188 – 192, 2000.

[10] K. Nishikawa, Y. Fujita, S. Uchida and H. Ohta, Effect of Surface Configuration on Nucleate Boiling Heat Transfer, *Int. J. Heat Mass Transfer*, vol. 27, pp. 1559-1571, 1984.

[11] S.M. You, T.W. Simon, A. Bar-Cohen, W. Tong, Experimental investigation of nucleate boiling incipience with a highly-wetting dielectric fluid (R-113), *Int. J. Heat Mass Transfer*, vol. 33, pp. 105–117, 1990.

[12] H.S. Liang, W.J. Yang, Nucleate pool boiling heat transfer in a highly-wetting liquid on micro-graphite-fiber composite surfaces, *Int. J. Heat Mass Transfer*, vol. 41, pp. 1993 – 2001, 1998.

[13] Y. Katto, S. Yokoya and K. Teraoka, Nucleate and Transition Boiling in a Narrow Space Between Two Horizontal, Parallel Disk Surfaces, *Bull. JSME*, vol. 20, pp. 638-643, 1977.

[14] X.F. Peng, H.Y. Hu, B.X. Wang, Boiling nucleation during liquid flow in microchannels, *International Journal of Heat and Mass Transfer*, vol.41, pp. 101-106, 1998.

[15] J.C. Passos, E.L. da Silva and L.F.B. Possamai, Visualization of FC72 Confined Nucleate Boiling, *Experimental Thermal and Fluid Science,* vol. 30, pp. 1-7, 2005.